
Representation Bayesian Risk Decompositions and Multi-Source Domain Adaptation

Xi Wu², Yang Guo¹, Jiefeng Chen¹, Yingyu Liang¹, Somesh Jha^{1,3}, and Prasad Chalasani³

¹University of Wisconsin-Madison

²Google

³XaiPient

Abstract

We consider representation learning (hypothesis class $\mathcal{H} = \mathcal{F} \circ \mathcal{G}$) where training and test distributions can be different. Recent studies provide hints and failure examples for domain invariant representation learning, a common approach for this problem, but the explanations provided are somewhat different and do not provide a unified picture. In this paper, we provide new decompositions of risk which give finer-grained explanations and clarify potential generalization issues. For Single-Source Domain Adaptation, we give an exact decomposition (an equality) of the target risk, via a natural hybrid argument, as sum of three factors: (1) source risk, (2) representation conditional label divergence, and (3) representation covariate shift. We derive a similar decomposition for the Multi-Source case. These decompositions reveal factors (2) and (3) as the precise reasons for failure to generalize. For example, we demonstrate that domain adversarial neural networks (DANN) attempt to regularize for (3) but miss (2), while a recent technique Invariant Risk Minimization (IRM) attempts to account for (2) but does not consider (3). We also verify our observations experimentally.

1 Introduction

Representation learning has emerged as a promising approach for machine learning in domain adaptation [5, 12] (for a more recent analysis of this line, see [14] and references therein). A common setup is to consider a hypothesis class \mathcal{H} that can be decomposed into $\mathcal{F} \circ \mathcal{G}$, where \mathcal{F} is a class of predictors which map representations to predictions¹, and \mathcal{G} is a class of representations which map inputs to representations. Compared to using a monolithic hypothesis class, using representations provides a new level of abstraction to study properties of information useful for adapting to different domains [6], including computer vision [26, 10] and natural language processing [9, 23].

A theme of representational domain adaptation is to derive a *risk decomposition* that involves representations, and use it to guide the search of desired representations. For example, a popular decomposition in single-source case is Domain Invariant Representations (DANN [12]):

$$R^t(f \circ \phi) \leq R^s(f \circ \phi) + d(\Phi^s, \Phi^t) + \lambda_{\mathcal{H}}^* \quad (1)$$

which says that target risk is bounded by three factors: (1) source risk, (2) distance between set of feature representations Φ^s and Φ^t , and (3) a term $\lambda_{\mathcal{H}}^*$ that solely depends on the overall hypothesis class \mathcal{H} (and thus is regarded as unlearnable).

However, recent work [14, 29, 2] has pointed out that the term $\lambda_{\mathcal{H}}^*$ hides information about different choices of representations, and thus may not be informative about the failure cases of domain invariant

¹In this work, we assume that the predictors output a probability vector over the labels, which corresponds to the output of softmax layer in typical classifiers, including deep neural networks.

representations. These works proposed failure examples and possible explanations (e.g., [14] proposed an explanation based on support misalignment). However, to some extent, these explanations are different from each other and do not give a unified picture.

In this paper we take a step to bridge this gap. We derive new risk decompositions that are more fine-grained and can clarify failure examples as precise terms in the decompositions. Our key idea is that since representation class \mathcal{G} provides an intermediate abstraction, it is fundamental to understand the following question: *What information does $\phi \in \mathcal{G}$ elicit for domain adaptation?*

1.1 Overview of our theory and results

As a first step to answer the question, we propose to examine the target risk where we equip over ϕ its Bayesian optimal predictor, and derive fine-grained risk decompositions. Our risk bounds show that explicitly incorporating representations can provide novel implications, and open an avenue for designing future algorithms for representation learning in domain adaptation. Our results can be broadly categorized into single-source and multi-source cases.

Single-Source Domain Adaptation (SSDA). We obtain the following results.

- We derive an *exact decomposition (an equality)* of the target risk, based on a natural hybrid argument, as three terms: (1) source risk, (2) representation conditional label divergence, and (3) representation covariate shift. We further give an exact decomposition of (3), based on Lebesgue decomposition, into (4) representation absolute continuous risk, and (5) representation singular risk.
- This equality allows us to identify a weakness of the invariant representation approach (DANN) as *mixing the effects of absolute continuous risk and singular risk, and may give inferior results due to intrinsic representation covariate shift*. It also allows us to explain failure examples as found in [14, 29] as exactly a large conditional divergence (factor (2)), and is information-theoretically impossible to solve without labeled data from the target distribution. This indicates that domain invariant representation approach (e.g. DANN) attempts to regularize (3) but misses (2), and there is a *fundamental limitation* of Single-Source Domain Adaptation with only *unlabeled* data from the target domain.
- We also analyze the *success* of DANN for MNIST \rightarrow MNIST-M² for which, similar to the failure example, the input support of two domains is disjoint. Our theory again gives an immediate explanation of this success: *The perfect representation alignment (i.e. factor (3) = 0) in this case trivially implies perfect conditional label alignment (i.e. factor (2) = 0)*.

Multi-Source Domain Adaptation (MSDA). We obtain the following results.

- Multiple training distributions allow us to observe conditional label divergence. We derive a risk decomposition that target risk is bounded by conditional label divergence and covariate shift in the training domains, plus a term called predictor adaptation distance quantifying whether these alignments in the source domains can generalize to the test domain.
- Our decomposition reveals that IRM [2] considers exactly perfect conditional label alignment (factor (2)), but misses representation covariate shift (factor (3)), and thus its performance may be hurt due to that, which is verified in our experiments (Figure 4). We further note that generalization to the target can fail when the predictor adaptation distance is large. We demonstrate this via an “distribution memorization problem” (Prop 1 and Section B.3).

Finally, we perform experiments to confirm our theoretical observations.

2 Preliminaries

Domain adaptation. Single-source domain adaptation has a source domain s and a target domain t . Each domain is a distribution over a set of feature vectors and labels. In the multi-source case, we have a set of source domains \mathcal{E}_{tr} , and one target domain e_0 for testing. Given a representation ϕ , we use Φ^e to denote the random vector $\phi(X^e)$ where X^e is the random variable distributed according to the input feature distribution in the environment e .

² Recall that MNIST-M is created by replacing the background of MNIST with colored images.

Cross entropy function and cross entropy loss. For simplicity of developing and presenting results, throughout this paper we will work with cross entropy loss. However, our results can be extended in a straightforward way to other loss functions. Given two distribution p, q , cross entropy function $H_p(q)$ is defined as $H_p(q) = \sum_i q_i \log \frac{1}{p_i}$. We also use cross entropy loss function where for a label $y \in [K]$, and a probability vector $p \in \Delta_K$, $\ell(p, y) = H_p(\mathbf{1}_y) = \log \frac{1}{p_y}$, where $\mathbf{1}_y$ is a K -dimensional vector with y -th component 1, and 0 otherwise. Given an environment e with distribution X^e, Y^e , and a hypothesis $h \in \mathcal{F} \circ \mathcal{G}$, we define its population risk over e , $R^e(h)$ as $\mathbb{E}[\ell(h(X^e), Y^e)]$.

Representation Bayesian optimal predictors. Given $\phi \in \mathcal{G}$, we denote by f_ϕ^e the Bayesian optimal predictor on top of the representation $\phi(X^e)$ in environment e . That is, $f_\phi^e(\gamma)$ outputs a probability vector such that for $y \in [K]$, $[f_\phi^e(\gamma)]_y = \Pr[Y^e = y | \phi(X^e) = \gamma]$. In other words, $f_\phi^e(\gamma) = (Y^e | \phi(X^e) = \gamma)$, the label distribution conditioned on $\phi(X^e) = \gamma$. To simplify notation, we simply use $Y^e | \gamma^e$.

3 Single-Source Domain Adaptation

Motivated by the central question (“What information does a representation elicit?”), we propose to examine the risk where we equip over ϕ its Bayesian optimal predictor.

3.1 An Exact Decomposition of Single-Source Representation Risk

The first step of our single-source decomposition is a hybrid argument based on a natural hybrid called s - t mixture. This hybrid distribution retains the same representation distribution as that of the target, but switches the label distribution conditioned on a representation to that of the source.

Definition 1 (s - t Mixture). An s - t mixture, denoted as (Φ^m, Y^m) , is a distribution defined on the $\Omega \times [K]$ (representation support times label space) as follows: (1) Φ^m and $\Phi^t = \phi(X^t)$ have the same distribution. That is the feature distribution follows the target domain. (2) On the other hand, $Y^m | \gamma^m = Y^s | \gamma^s$. That is, the conditional label distribution follows the source domain.

This mixture gives rise to some natural quantities for risk decomposition. We first consider *representation conditional label divergence*. Given a representation ϕ , and a value γ that ϕ may take, the conditional label distributions $Y^t | \gamma^t$ and $Y^s | \gamma^s$ may differ. We introduce two notions,

Definition 2 (Representation Domain KL-Divergence). We define (representation) domain KL-divergence as $\text{KL}_\phi^{s,t} := \int_\Omega d_{\text{KL}}(f_\phi^t(\gamma) \| f_\phi^s(\gamma)) \mu^t(d\gamma)$. where d_{KL} is the KL divergence. Importantly, this quantity is natural since it is exactly $R^t(f_\phi^s \circ \phi) - R^t(f_\phi^t \circ \phi)$: The gap of target risk if we switch predictor from f_ϕ^t (target optimal) to f_ϕ^s (source optimal).

Definition 3 (Representation Domain Bayesian Divergence). We define (representation) domain Bayesian divergence as $\delta_\phi^{s,t} := \int_\Omega (\mathbb{H}(Y^t | \gamma^t) - \mathbb{H}(Y^s | \gamma^s)) \mu^t(d\gamma)$. Importantly, this quantity is natural since it is exactly $R^t(f_\phi^t \circ \phi) - R^m(f_\phi^s \circ \phi)$: The gap between the risks on the target and mixture distribution (recall that target and mixture share the same representation distributions; f_ϕ^t is optimal for the target, and f_ϕ^s is optimal for the mixture).

We refer readers to [24] for a detailed study of the relationship between the two notions above. Symmetrically, we can consider fixing the conditional label distributions, but vary the underlying representation distribution. This gives *representation covariate shift*:

Definition 4 (Representation Covariate Shift). We define s - t representation covariate shift, denoted as $\mu_\phi^{s,t}$, as $\mu_\phi^{s,t} = \int_\Omega \mathbb{H}(Y^s | \gamma^s) \mu^t(d\gamma) - \int_\Omega \mathbb{H}(Y^s | \gamma^s) \mu^s(d\gamma)$. In other words, we consider representation distribution changing from Φ^s to Φ^t , while fixing conditional label distribution as $Y^s | \gamma^s$.

Lemma 1 (Exact decomposition into conditional divergence and covariate shift). We have that

$$R^t(f_\phi^s \circ \phi) = \underbrace{R^s(f_\phi^s \circ \phi)}_{\text{source error}} + \underbrace{\text{KL}_\phi^{s,t} + \delta_\phi^{s,t}}_{\text{conditional label div}} + \underbrace{\mu_\phi^{s,t}}_{\text{covariate shift}} \quad (2)$$

We next give an *exact* decomposition of the representation covariate shift $\mu_\phi^{s,t}$. By the Lebesgue decomposition theorem [25], we know that $\mu^t = \mu_0^t + \mu_1^t$ where $\mu_0^t \ll \mu^s$ is a measure that is

absolutely continuous in μ^s and μ_1^t is a measure that is singular in μ^s . This decomposition has a natural interpretation in view of domain adaptation: μ_0^t represents the target representations that can be observed in μ^s , whereas μ_1^t represents the target representations that *cannot* be observed via μ^s . For μ_0^t , by the Radon-Nykodym theorem, we have then a function $\omega_\phi(\cdot) \equiv \frac{d\mu_0^t}{d\mu^s} : \mathbb{R}^k \mapsto \mathbb{R}$, so that for any measurable set B : $\mu_0^t(B) = \int_B \omega_\phi(\gamma) d\mu^s(\gamma)$. We thus introduce two notions.

Definition 5 (Representation Singular Risk). Let $\tau_\phi^{s,t} \equiv \tau_\phi^{s,t}(\mu_1^t) \equiv \int_\Omega H(Y^s | \gamma^s) \mu_1^t(d\gamma)$.

Definition 6 (Representation Absolute Continuous Risk). Let

$$\zeta_\phi^{s,t} \equiv \zeta_\phi^{s,t}(\mu_0^t) \equiv \int_\Omega (\omega_\phi(\gamma) - 1) H(Y^s | \gamma^s) \mu^s(d\gamma)$$

Lemma 2 (Exact decomposition of representation covariate shift). $\mu_\phi^{s,t} = \zeta_\phi^{s,t} + \tau_\phi^{s,t}$.

Combining the above two lemmas we thus arrive at the main theorem for the single-source case:

Theorem 1 (Exact Decomposition of Single-Source Risk). We have that

$$R^t(f_\phi^s \circ \phi) = \underbrace{R^s(f_\phi^s \circ \phi)}_{\text{source error}} + \underbrace{\text{KL}_\phi^{s,t} + \delta_\phi^{s,t}}_{\text{conditional label div}} + \underbrace{\zeta_\phi^{s,t}}_{\text{absolute continuous risk}} + \underbrace{\tau_\phi^{s,t}}_{\text{singular risk}} \quad (3)$$

3.2 Comparison with existing risk decompositions

DANN and intrinsic representation covariate shift. One can contrast DANN decomposition (1) with our fine-grained decomposition, in particular (2). One can see that for common distribution distance function $d(\cdot, \cdot)$ (e.g., MMD), $d(\Phi^s, \Phi^t)$ mixes the effect of absolute continuous risk and singular risk. More precisely, even if the singular part becomes zero for a “right” representation, there might be nontrivial absolute continuous risk because there is *intrinsic* covariate shift from μ^s to μ_0^t . In this situation, *even if we discover the right representation ϕ , $d(\Phi^s, \Phi^t)$ may still be significant and DANN may excessively modify ϕ in order to reduce $d(\Phi^s, \Phi^t)$, leading to adverse results.*

In fact, some recent proposals (for example, [16]) made similar observations, and they considered modifying (1) to align the conditional representation distributions, $\Phi^s | Y^s$ and $\Phi^t | Y^t$, instead of Φ^s and Φ^t . However, in view of our results, this is only one form of intrinsic covariate shift, and one can easily modify the representation distributions to break these variants.

Comparison with other bounds. We now consider other representative decompositions, specifically: (T1) Theorem 1 [4], (T2) Theorem 4.1 [29], and (T3) Theorem 2 [14]. More related work are discussed in Sections E and F. To begin with, the Bayes classifier and our other notions (Def 2 to 4) are defined w.r.t. the representation. For both (T1) and (T2), the notions are w.r.t. the input space (e.g., “Notations” and “Comparison with Theorem 2.1” in [29]). Working at representation level allows us to examine different representation conditional distributions in a hypothesis class of representations. (T1) and (T2) do not formulate representation class. Our bound is tighter even if one applies (T1) and (T2) at the representation level. This is because an equality implies that our terms must be reflected in any valid upper bound, but still, an equality can provide more thorough insights. For (T1), we provide a detailed comparison in Appendix F. The insufficiency of (T1) has also been discussed in several existing works (including [29, 14]).

For (T2), we note two more points: (i) Our decomposition is an “orthogonal decomposition” but (T2) is not. Specifically, our conditional label divergence terms (Def 2 and 3) are not affected by representation covariate shift since both integrals are only evaluated over the target representation distribution. By contrast, while the third term in (T2) is related to conditional label divergence, it depends on both source and target representation distributions, and so mixes conditional label divergence and covariate shift. (ii) While the second term in (T2) can be interpreted as covariate shift over representations, our term provides a precise characterization of the effect of absolute continuous and singular risks, unveiling a weakness of DANN.

(T3) is the closest decomposition to ours. However their decomposition is not exact and indeed upper bounds our absolute continuous risk and singular risk. This again demonstrates the benefits of our equality decomposition.

Controlling covariate shift via source fairness. In Section A.3 we derive an upper bound of the representation covariate shift that has algorithmic implications. In that upper bound we consider a

notion called *representation source fairness*, which encourages to find a representation ϕ that has uniform performance across different representations γ . The notion only depends on the source domain, and can thus be learned with labeled source data. We note that this notion generalizes a similar theme considered in recent work [11] to the representation level.

3.3 Analysis of examples of domain invariant representations

We now use our theory to analyze two examples of Domain Invariant Representations.

Example 1 (A failure example from [14, 29]). Consider input space $X = [-1, 1] \times [-1, 1]$, $\mathcal{G} = \{\phi_1, \phi_2\}$ where $\phi_1(x) = x_1$ and $\phi_2(x) = x_2$, and $\mathcal{F} = \{\mathbf{1}_\lambda(\cdot)\}$ (that is we consider thresholding functions that $\mathbf{1}_\lambda(\alpha) = 1$ if $\alpha > \lambda$, and 0 otherwise). The source domain s puts a uniform distribution in the second and fourth quadrants, and has label 1 in the second quadrant, and label 0 in the fourth quadrant. On the other hand, target distribution t puts a uniform distribution in the first and third quadrant, and has label 1 in the first quadrant and label 0 in the third quadrant (See Figure 1). Clearly, the underlying truth is $\phi_2(x) = x_2$, which perfectly classifies both source and target data. However, with only unlabeled data from the target domain, using (1) we cannot distinguish between ϕ_1 and ϕ_2 : Both of them have zero risk on the source domain, and both give perfect alignment between Φ^s and Φ^t . (i.e., both perfectly minimize (1)).

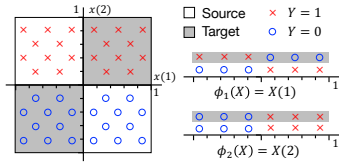


Figure 1: Example from [14] where DANN fails to learn. (1) has two different source-optimal solutions with different target risks. The figure is from [14].

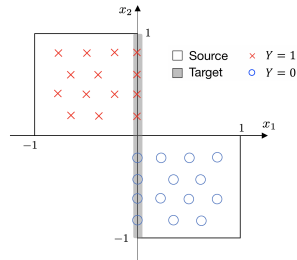


Figure 2: The source domain is the same, but the target domain has $x_1 = 0$.

Our explanation using conditional label divergence. Theorem 1 provides an immediate explanation for Example 1: ϕ_1 has a large representation conditional label divergence. Since we only have one source domain, and do not have labeled data from the target domain, it is information theoretically impossible to align conditional label distributions, and thus distinguish between ϕ_1 and ϕ_2 . We note that [29] mentioned a similar explanation based on their Theorem 4.1. As we have discussed in the previous section, our exact decomposition at representation level provides a more precise explanation (zero representation covariate shift but large conditional label divergence).

Example 2 (An example on which DANN succeeds). We consider the same setting as in Example 1. However, for target domain, we have uniform distribution over $\{0\} \times [-1, 1]$, and for $\{(0, x_2) \mid 0 < x_2 < 1\}$ we give label 1, and for $\{(0, x_2) \mid -1 < x_2 < 0\}$ we give label 0. In other words, the probability mass, instead of spreading over the second and the fourth quadrants, it concentrates on the x_2 axis. In this case, only $\phi_2(x) = x_2$ aligns the representation distributions, since $\phi_1(x) = x_1$ will be constantly 0 for the unlabeled data from the target domain, which has measure 0 in the source data when projecting to x_1 . DANN will thus learn x_2 which perfectly classifies the target data.

The success of DANN on MNIST→MNIST-M. The example above captures the essence of the success of DANN on MNIST→MNIST-M: The representation alignment in this case trivially implies conditional label alignment. Merely replacing background images will make digit representation the only discriminative signal that exists in both source and target. Therefore by finding the only representation that could align the two domains, the conditional label alignment is trivially implied.

4 Multi-Source Domain Adaptation

We now switch to the setting with multiple sources. Multiple source domains allow us to observe conditional label divergence among source domains, which one cannot hope to do with a single

source (without labeled target data). Due to the availability of multiple source domains, we focus on the case where no data (labeled or unlabeled) from the target domain is available for training.

4.1 Multi-Source Representation Risk Decomposition

We observe that, even with multiple source domains, generalization to a target domain requires connections between the target and sources. For this we introduce *Predictor Adaptation Gap*.

Definition 7 (Predictor adaption gap between two distributions). Define the predictor adaptation gap between two distributions e_1 and e_2 with respect to a representation function ϕ and \mathcal{E}_{tr} as $d_\phi(e_1, e_2; \mathcal{E}_{\text{tr}}) \equiv \sup_{e \in \mathcal{E}_{\text{tr}}} R^{e_1}(f_\phi^e \circ \phi) - R^{e_2}(f_\phi^e \circ \phi)$. Intuitively, a small gap indicates that a small $R^{e_2}(f_\phi^e \circ \phi)$ implies small $R^{e_1}(f_\phi^e \circ \phi)$. That is, $f_\phi^e \circ \phi$ can be used in e_1 .

Definition 8 (Predictor adaptation gap between target and sources). Define the predictor adaptation gap between e_0 and \mathcal{E}_{tr} with respect to ϕ as: $d_\phi(e_0, \mathcal{E}_{\text{tr}}) \equiv \inf_{e' \in \mathcal{E}_{\text{tr}}} d_\phi(e_0, e'; \mathcal{E}_{\text{tr}})$. We also define the predictor adaptation gap between e_0 and \mathcal{E}_{tr} over the whole class \mathcal{G} as $d_{\mathcal{G}}(e_0, \mathcal{E}_{\text{tr}}) \equiv \sup_{\phi \in \mathcal{G}} d_\phi(e_0, \mathcal{E}_{\text{tr}})$.

Theorem 2 (Multi-Source Risk Decomposition). For any ϕ , we have

$$\sup_{e \in \mathcal{E}_{\text{tr}}} R^{e_0}(f_\phi^e \circ \phi) \leq \underbrace{\sup_{e \in \mathcal{E}_{\text{tr}}} R^e(f_\phi^e \circ \phi)}_{\text{source error}} + \underbrace{\sup_{e, e' \in \mathcal{E}_{\text{tr}}} [\delta_\phi^{e, e'} + \text{KL}_\phi^{e, e'} + \mu_\phi^{e, e'}]}_{\text{cond. label div. + covariate shift}} + \underbrace{d_\phi(e_0, \mathcal{E}_{\text{tr}})}_{\text{predictor adaptation gap}}. \quad (4)$$

Compared with Theorem 1, Theorem 2 has an additional term of predictor adaptation gap. This is intentional since the predictor gap is related to the target and thus cannot be optimized in the setting without target data. Importantly, this bound shows a trade-off between the generalization gap and the other two terms: A larger \mathcal{E}_{tr} may lead to a smaller gap but larger source risks, larger label divergence and covariate shift among the sources, and harder optimization. Similarly, the bound also shows a larger hypothesis class \mathcal{G} potentially leads to smaller source risks but a larger gap. To see this, suppose the optimization method successfully finds a $\hat{\phi}$ with small source risks, and small conditional label divergence and covariate shift among the sources. Then, the generalization gap is $d_{\hat{\phi}}(e_0, \mathcal{E}_{\text{tr}})$, which can be as large as $\sup_{\phi \in \mathcal{G}} d_\phi(e_0, \mathcal{E}_{\text{tr}})$ in the worst case.

4.2 Conditional Label Divergence and Invariant Risk Minimization

We consider the following notion for regularizing conditional divergence.

Definition 9 (Environment Conditional Invariance). A representation ϕ satisfies environment conditional invariance (ECI) w.r.t. distribution family \mathcal{E} if $\forall e, e' \in \mathcal{E}, \forall r \in \text{supp}(\phi(X^e)) \cap \text{supp}(\phi(X^{e'}))$, $\forall y \in [K], \Pr[Y^e = y | \phi(X^e) = r] = \Pr[Y^{e'} = y | \phi(X^{e'}) = r]$.

ECI means that the Bayesian optimal prediction function on the representation (i.e., $\Pr[Y^e | \phi(X^e)]$) is invariant across all the distributions. This notion is closely related to the notion of invariant prediction in [22], and has been mentioned in recent work (e.g., [20]). Furthermore, a recent work [2] of Invariant Risk Minimization (IRM) has proposed and studied a closely related notion that representation ϕ leads to the existence of a predictor *simultaneously optimal* for all the domains:

$$\begin{aligned} & \min_{h \in \mathcal{F}, \phi \in \mathcal{G}} \sum_{e \in \mathcal{E}_{\text{tr}}} R^e(h \circ \phi), \\ & \text{subject to } h \in \arg \min_{h \in \mathcal{F}} R^e(h \circ \phi) \quad \text{for } \forall e \in \mathcal{E}_{\text{tr}}. \end{aligned} \quad (5)$$

ECI and IRM are not equivalent if the loss (e.g., 0-1 loss) does not have the property that the minimizer is the Bayesian optimal predictor.³ If the loss function satisfies the Bayesian optimality property, and the hypothesis class \mathcal{F} contains the Bayes predictor of representations, ECI and IRM are equivalent. In this case, let \mathcal{G}_I denote the subset of hypotheses in \mathcal{G} that satisfy ECI. Then IRM is equivalent to minimizing $\sum_{e \in \mathcal{E}_{\text{tr}}} R_e(h \circ \phi)$ subject to $h \in \mathcal{F}, \phi \in \mathcal{G}_I$. By Theorem 2, the solution $\hat{h} \circ \hat{\phi}$ satisfies

$$R^{e_0}(\hat{h} \circ \hat{\phi}) \leq \sup_{e \in \mathcal{E}_{\text{tr}}} R^e(\hat{h} \circ \hat{\phi}) + \sup_{e, e' \in \mathcal{E}_{\text{tr}}} \mu_\phi^{e, e'} + d_{\mathcal{G}_I}(e_0, \mathcal{E}_{\text{tr}}). \quad (6)$$

Compared to the original bound, ECI enforces perfect conditional label alignment, and also potentially reduces the generalization gap from $d_{\mathcal{G}}(e_0, \mathcal{E}_{\text{tr}})$ to $d_{\mathcal{G}_I}(e_0, \mathcal{E}_{\text{tr}})$ by pruning away those hypothesis ϕ that do not satisfy ECI on the sources. When the ground-truth indeed satisfies ECI, this will not hurt the sources risks and thus significantly decreases the bound on the target risk.

³ See Section C for a detailed discussion. Therefore, we use ECI for our analysis, since it is a property of the representation itself and does not involve the optimization and thus is more convenient for the analysis.

4.3 Predictor Adaptation Gap

In this section we study the problem of *distribution memorization* that may lead to a large predictor adaptation gap. Distribution memorization is similar to overfitting via memorizing training samples in the traditional supervised learning setting, but it memorizes the entire distributions rather than the training samples. Even if infinite data from each source is available and the hypothesis classes are just slightly larger than necessary, distribution memorization can happen. To illustrate this, we consider the following example: Consider the case with classification error, i.e., the label is in $\{-1, +1\}$ and the loss of f on data (x, y) is $\ell(f(x), y) = |\text{sign}(f(x)) - y|$. Suppose the support of the target $\text{supp}(X^{\text{to}})$ can be disjoint from those of the sources $\cup_{e \in \mathcal{E}_s} \text{supp}(X^e)$. Assume: (1) There are ground-truth $\phi^* \in \mathcal{G}$ and $f^* \in \mathcal{F}$, such that $f^* \circ \phi^*$ has 0 error in all domains (including all sources and also the target), ϕ^* satisfies ECI in all domains, and the distributions of $\phi^*(X^e)$ are the same for all sources e . (2) The optimization finds f and ϕ such that in all sources, $f \circ \phi$ has 0 error, ϕ satisfies ECI, and the distributions of $\phi(X^e)$ are the same.

Proposition 1 (Distribution Memorization). *There exists an instance of the data distributions and $\mathcal{G} \circ \mathcal{F}$ satisfying the above assumptions, where there is an optimal solution $f \circ \phi$ that satisfies ECI and has 0 risks in all the source domains, but in the target domain has a risk $1/2$ which is as large as random guessing. Furthermore, in the instance, $\phi(x)$ is simply the concatenation of $\phi^*(x)$ with one additional bit, and f is linear.*

Intuitively, the representation remembers whether the data is from the target and then the predictor uses this to make different predictions for the target domain. More generally, we do not need the support of the target domain to be disjoint from those of the source domains. A similar phenomena can happen when the target has large total variation distances with the sources and the hypothesis classes are too large.⁴ Our analysis shows that the representation class should be carefully chosen to alleviate the prediction adaptation gap and consequently get better generalization to the target domain. The connection between the prediction adaptation gap and the label divergence and covariate shift (between target and sources) also suggests that if some (unlabeled) data from the target domain are available, such data can potentially be used to regularize the gap explicitly during the training.

5 Experiments

In this section we perform experiments to verify our theoretical observations.

SSDA: Representation covariate shift. We demonstrate two points: (1) Without considering representation covariate shift, DANN performance will deteriorate with more significant covariate shift. (2) More importantly, we demonstrate a novel point inspired by our theory that, if we “reweigh” the points according to the covariate shift (i.e., we have an oracle which tells us the representation covariate shift for the right representation), then DANN works again.

To do so, we follow the MNIST \rightarrow MNIST-M domain adaptation scenario from [12]. To induce representation covariate shift, the data in the target domain are skewly sampled for each class according to a weight vector w . w is set as follows: (1) Mild covariate shift case: $\omega[i] = 0.25$ if $i = 0$, $\omega[i] = 9$ if $i = 9$, and otherwise $\omega[i] \sim \text{Uniform}([.25, .75])$. (2) Strong covariate shift case: $\omega[i] = 0.0625$ if $i = 0$, $\omega[i] = 0.9375$ if $i = 9$, and otherwise $\omega[i] \sim \text{Uniform}([.0625, .9375])$.

Figure 3 confirms the gap in the target accuracy between naive application of DANN and DANN with oracle source sampling is significant: It increases with the effect of representation covariate, which is measured by the maximum relative weight ratio in our case. This gap confirms our theoretical observation that *DANN objectives mix the effect of absolute continuous and singular risks, which can result in inferior performance*. This also suggests that the design of domain adaptation algorithms may need to consider separating the effect of absolute continuous and singular risks.

MSDA: IRM and source-target representation covariate shift. Our analysis indicates a large representation distribution shift can lead to larger target risks, and only enforcing ECI will not suffice. Here we provide supporting empirical evidence, by experimenting on a variant of the colored MNIST dataset from [2]. In the original construction, we have equal mass on the digits in both source

⁴ Section B.3 provides a more complex example where the supports of the target and the sources overlap but a large representation covariate shift leads to a large gap. It also provides another example where the supports overlap while a large conditional label divergence leads to a large gap.

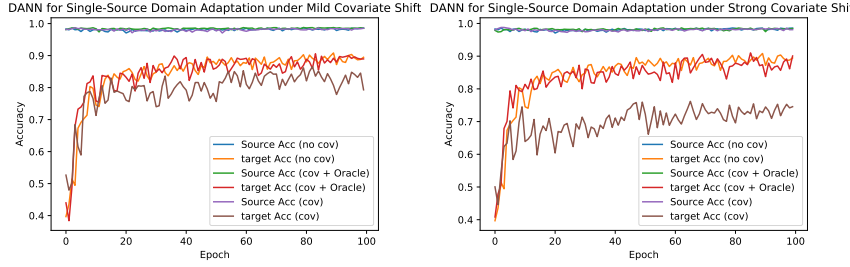


Figure 3: Source and Target accuracy for DANN under mild (Left) and strong covariate shift (right). In each scenario, we compare three cases: no covariate shift (baseline), covariate shift with naive DANN, covariate shift with DANN under oracle sampling for the source domain

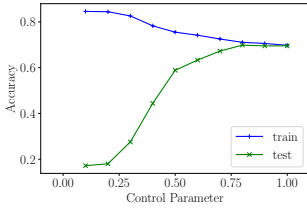


Figure 4: IRM under representation covariate shift. Smaller control parameter gives larger representation covariate shift, and worse test accuracy.

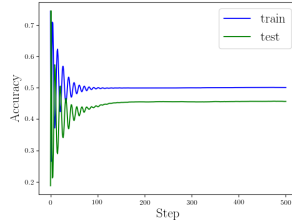


Figure 5: Training and test accuracy of IRMv1 v.s. epochs. Left: one-stage, use the regularization to impose ECI for the whole training. Right: two-stage, first train without the regularization for 190 steps and then use regularization. One can see that the two stage training significantly improves the test accuracy.

domains, so there is no representation covariate shift. We modify the construction process so that the two source domains have *misaligned* distributions over the digits: e_1 has mass $\frac{p}{1+p}$ on digits 0-4 and $\frac{1}{1+p}$ on digits 5-9, while e_2 has mass $\frac{1}{1+p}$ on digits 0-4 and $\frac{p}{1+p}$ on digits 5-9. So the shift is controlled by a single control parameter p , as p increases the shift becomes larger. Figure 4 shows the results where p increases the test accuracy continues to decrease.⁵ The result confirms our observation that as the representation covariate shift becomes more significant, models learned on the source domains have worse generalization to the test domain.

MSDA: IRM, hypothesis class size, and predictor adaptation gap. [2] proposed an algorithm called IRMv1 for IRM. We observe that, IRMv1 *fails* to generalize on Color-MNIST when imposing the ECI regularization for the *whole* training process. On the other hand, a two-stage training succeeds: First we train without regularization, and then train with the regularization. Figure 5 gives the learning curves for these two training methods. For this interesting observation, our multi-source theory provides an explanation that, essentially, *the first stage is a pretraining which gives a smaller hypothesis class that may have smaller predictor adaption gap*. More precisely, the first stage begins with an initialization ϕ_0 and finds an intermediate solution ϕ_1 , and the second stage uses ϕ_1 as a warm start and searches in a neighborhood $\mathcal{N}(\phi_1)$ of ϕ_1 to obtain the final solution ϕ_2 . Here, $\mathcal{N}(\phi_1)$ can be much smaller than the original hypothesis class \mathcal{G}_I . Then the predictor adaptation gap reduces from $d_{\mathcal{G}_I}(e_0, \mathcal{E}_T)$ to $d_{\mathcal{N}(\phi_1)}(e_0, \mathcal{E}_T)$, and thus improves generalization. We confirmed this explanation empirically. We computed the ℓ_2 distance between the parameters of ϕ_0 and ϕ_1 , and for ϕ_1 and ϕ_2 . The latter is less than 8% of the former, suggesting that it is indeed doing pre-training and supporting our explanation. This also suggests that *the two-stage training heuristic can be a general strategy to improve generalization in domain adaptation*.

⁵ The exact data generating process and results are provided in Appendix D and Table 1.

6 Broader Impact

This paper is purely theoretical and has no immediate societal impact. It may lead to the development of better domain adaptation algorithms, which may have practical impact.

References

- [1] H. Ajakan, P. Germain, H. Larochelle, F. Laviolette, and M. Marchand. Domain-adversarial neural networks. *stat*, 1050:15, 2014.
- [2] M. Arjovsky, L. Bottou, I. Gulrajani, and D. Lopez-Paz. Invariant risk minimization. *CoRR*, abs/1907.02893, 2019.
- [3] K. Azizzadenesheli, A. Liu, F. Yang, and A. Anandkumar. Regularized learning for domain adaptation under label shifts. *arXiv preprint arXiv:1903.09734*, 2019.
- [4] S. Ben-David, J. Blitzer, K. Crammer, A. Kulesza, F. Pereira, and J. W. Vaughan. A theory of learning from different domains. *Machine learning*, 79(1-2):151–175, 2010.
- [5] S. Ben-David, J. Blitzer, K. Crammer, and F. Pereira. Analysis of representations for domain adaptation. In B. Schölkopf, J. C. Platt, and T. Hofmann, editors, *Advances in Neural Information Processing Systems 19, Proceedings of the Twentieth Annual Conference on Neural Information Processing Systems, Vancouver, British Columbia, Canada, December 4-7, 2006*, pages 137–144. MIT Press, 2006.
- [6] Y. Bengio, A. Courville, and P. Vincent. Representation learning: A review and new perspectives. *IEEE transactions on pattern analysis and machine intelligence*, 35(8):1798–1828, 2013.
- [7] J. Blitzer, K. Crammer, A. Kulesza, F. Pereira, and J. Wortman. Learning bounds for domain adaptation. In *Advances in neural information processing systems*, pages 129–136, 2008.
- [8] N. Courty, R. Flamary, A. Habrard, and A. Rakotomamonjy. Joint distribution optimal transportation for domain adaptation. In *Advances in Neural Information Processing Systems*, pages 3730–3739, 2017.
- [9] J. Devlin, M.-W. Chang, K. Lee, and K. Toutanova. Bert: Pre-training of deep bidirectional transformers for language understanding. *arXiv preprint arXiv:1810.04805*, 2018.
- [10] A. Dosovitskiy and T. Brox. Inverting visual representations with convolutional networks. In *Proceedings of the IEEE conference on computer vision and pattern recognition*, pages 4829–4837, 2016.
- [11] J. Duchi and H. Namkoong. Learning models with uniform performance via distributionally robust optimization. *arXiv preprint arXiv:1810.08750*, 2018.
- [12] Y. Ganin, E. Ustinova, H. Ajakan, P. Germain, H. Larochelle, F. Laviolette, M. Marchand, and V. Lempitsky. Domain-adversarial training of neural networks. *The Journal of Machine Learning Research*, 17(1):2096–2030, 2016.
- [13] M. Gong, K. Zhang, T. Liu, D. Tao, C. Glymour, and B. Schölkopf. Domain adaptation with conditional transferable components. In *International conference on machine learning*, pages 2839–2848, 2016.
- [14] F. D. Johansson, D. A. Sontag, and R. Ranganath. Support and invertibility in domain-invariant representations. In *The 22nd International Conference on Artificial Intelligence and Statistics, AISTATS 2019, 16-18 April 2019, Naha, Okinawa, Japan*, pages 527–536, 2019.
- [15] D. Kifer, S. Ben-David, and J. Gehrke. Detecting change in data streams. In *VLDB*, volume 4, pages 180–191. Toronto, Canada, 2004.
- [16] Y. Li, X. Tian, M. Gong, Y. Liu, T. Liu, K. Zhang, and D. Tao. Deep domain generalization via conditional invariant adversarial networks. In *Computer Vision - ECCV 2018 - 15th European Conference, Munich, Germany, September 8-14, 2018, Proceedings, Part XV*, volume 11219 of *Lecture Notes in Computer Science*, pages 647–663. Springer, 2018.
- [17] M. Long, Y. Cao, J. Wang, and M. I. Jordan. Learning transferable features with deep adaptation networks. *arXiv preprint arXiv:1502.02791*, 2015.

- [18] M. Long, J. Wang, G. Ding, J. Sun, and P. S. Yu. Transfer joint matching for unsupervised domain adaptation. In *Proceedings of the IEEE conference on computer vision and pattern recognition*, pages 1410–1417, 2014.
- [19] Y. Mansour, M. Mohri, and A. Rostamizadeh. Multiple source adaptation and the rényi divergence. In *Proceedings of the Twenty-Fifth Conference on Uncertainty in Artificial Intelligence*, pages 367–374, 2009.
- [20] S. J. Pan, I. W. Tsang, J. T. Kwok, and Q. Yang. Domain adaptation via transfer component analysis. *IEEE Transactions on Neural Networks*, 22(2):199–210, 2010.
- [21] Z. Pei, Z. Cao, M. Long, and J. Wang. Multi-adversarial domain adaptation. In *Thirty-Second AAAI Conference on Artificial Intelligence*, 2018.
- [22] J. Peters, P. Bühlmann, and N. Meinshausen. Causal inference using invariant prediction: identification and confidence intervals. *arXiv e-prints*, page arXiv:1501.01332, Jan 2015.
- [23] M. E. Peters, M. Neumann, M. Iyyer, M. Gardner, C. Clark, K. Lee, and L. Zettlemoyer. Deep contextualized word representations. *arXiv preprint arXiv:1802.05365*, 2018.
- [24] D. Reeb and M. M. Wolf. Tight bound on relative entropy by entropy difference. *IEEE Trans. Inf. Theory*, 61(3):1458–1473, 2015.
- [25] W. Rudin. *Real and complex analysis*. Tata McGraw-hill education, 2006.
- [26] O. Sener, H. O. Song, A. Saxena, and S. Savarese. Learning transferrable representations for unsupervised domain adaptation. In *Advances in Neural Information Processing Systems*, pages 2110–2118, 2016.
- [27] J. Shen, Y. Qu, W. Zhang, and Y. Yu. Wasserstein distance guided representation learning for domain adaptation. In *Thirty-Second AAAI Conference on Artificial Intelligence*, 2018.
- [28] K. Zhang, B. Schölkopf, K. Muandet, and Z. Wang. Domain adaptation under target and conditional shift. In *International Conference on Machine Learning*, pages 819–827, 2013.
- [29] H. Zhao, R. T. des Combes, K. Zhang, and G. J. Gordon. On learning invariant representations for domain adaptation. In *Proceedings of the 36th International Conference on Machine Learning, ICML 2019, 9-15 June 2019, Long Beach, California, USA*, pages 7523–7532, 2019.
- [30] H. Zhao, S. Zhang, G. Wu, J. M. Moura, J. P. Costeira, and G. J. Gordon. Adversarial multiple source domain adaptation. In *Advances in neural information processing systems*, pages 8559–8570, 2018.

A Proofs for Section 3

A.1 Proof of Lemma 1

We decompose $R^t(f_\phi^s \circ \phi) - R^s(f_\phi^s \circ \phi)$ as

$$\begin{aligned} R^t(f_\phi^s \circ \phi) - R^s(f_\phi^s \circ \phi) &= \left(R^t(f_\phi^s \circ \phi) - R^t(f_\phi^t \circ \phi) \right) \\ &+ \left(R^t(f_\phi^t \circ \phi) - R^m(f_\phi^s \circ \phi) \right) \\ &+ \left(R^m(f_\phi^s \circ \phi) - R^s(f_\phi^s \circ \phi) \right). \end{aligned}$$

One can then verify that $R^t(f_\phi^s \circ \phi) - R^t(f_\phi^t \circ \phi) = \text{KL}_{\phi}^{s,t}$, $R^t(f_\phi^t \circ \phi) - R^m(f_\phi^s \circ \phi) = \delta_{\phi}^{s,t}$, $R^m(f_\phi^s \circ \phi) - R^s(f_\phi^s \circ \phi) = \mu_{\phi}^{s,t}$.

A.2 Proof of Lemma 2

Note that $\mu_{\phi}^{s,t} = \int_{\Omega} H(Y^s | \gamma^s) \mu^t(d\gamma) - \int_{\Omega} H(Y^s | \gamma^s) \mu^s(d\gamma) = \int_{\Omega} H(Y^s | \gamma^s) \mu_0^t(d\gamma) - \int_{\Omega} H(Y^s | \gamma^s) \mu^s(d\gamma) + \tau_{\phi}$. Further, $\int_{\Omega} H(Y^s | \gamma^s) \mu_0^t(d\gamma) - \int_{\Omega} H(Y^s | \gamma^s) \mu^s(d\gamma) = \int_{\Omega} (\omega_{\phi}(\gamma) - 1) H(Y^s | \gamma^s) \mu^s(d\gamma) = \zeta_{\phi}$

A.3 Upper Bounding Representation Covariate Shift via Source Fairness

In this section we study a bound on the representation covariate shift $\mu_{\phi}^{s,t}$ that has algorithmic implications. For ease of notations we assume that there is no the singular part, but the argument here can be easily extended to the situation with nontrivial singular part.

Point Fairness. We consider the following definition:

Definition 10 (Representation Source Fairness). *The representation source fairness ρ_{ϕ}^s is defined as $\rho_{\phi}^s \equiv \sup_{\gamma \in \Omega} \{H(Y^s | \gamma^s)\}$.*

Source fairness quantifies the intrinsic difficulties of ϕ in discriminating certain inputs (that is, even the Bayesian optimal predictor over ϕ cannot discriminate the inputs mapped to γ well). Intuitively, if ϕ is good at discriminating some inputs, but very bad at some others, then ϕ is unfair to those inputs (even though they may only occur with very small probability).

We note that, importantly, this quantity *only* depends on the *source domain*, and so it is learnable using labeled source data. Finally, observe that $\rho_{\phi}^s \leq \log K$, where the maximal is achieved when $Y^s | \gamma$ is a uniform distribution over $[K]$. This leads to the following bound on covariate shift.

Theorem 3.

$$\mu_{\phi}^{s,t} \leq \underbrace{\rho_{\phi}^s}_{\text{repr. source fairness}} \times \underbrace{d_{\text{TV}}(\Phi^s, \Phi^t)}_{\text{repr. divergence}}$$

Proof. Note that $\kappa(\gamma) := H(Y^s | \gamma^s) / \rho_{\phi}^s$ is a function bounded by 1, and $\mu_{\phi}^{s,t}$ is indeed $\rho_{\phi}^s \cdot \left(\int_{\Omega} \kappa(\gamma) \mu^t(d\gamma) - \int_{\Omega} \kappa(\gamma) \mu^s(d\gamma) \right)$, which is bounded by $\rho_{\phi}^s \cdot d_{\text{TV}}(\Phi^s, \Phi^t)$ where $d_{\text{TV}}(\Phi^s, \Phi^t)$ is the total variation distance between Φ^s and Φ^t . \square

Group Fairness. We can tighten the previous bound based on group fairness instead of point-wise fairness. Let \mathcal{B} be a partition of the space of the representation ϕ . Assume for simplicity $|\mathcal{B}|$ is finite.

Definition 11 (Group Representation Source Fairness). *The group (representation) source fairness $\rho_{\phi, \mathcal{B}}^s$ with respect to \mathcal{B} is defined as $\rho_{\phi, \mathcal{B}}^s := \sup_{B \in \mathcal{B}'} \{H(Y^s | \Phi^s \in B)\}$, where $\mathcal{B}' = \{B \in \mathcal{B} : \Pr[\Phi^s \in B] > 0\}$.*

Definition 12 (Group Distance). *The group distance between two distributions μ and ν with respect to \mathcal{B} is defined as $d_{\mathcal{B}}(\mu, \nu) = \frac{1}{2} \sum_{B \in \mathcal{B}} |\mu(B) - \nu(B)|$.*

Theorem 4. Suppose Φ^t is supported on Φ^s , i.e., if $\Pr[\Phi^t \in B] > 0$ for some set B , then $\Pr[\Phi^s \in B] > 0$. Then we have

$$\begin{aligned}\mu_\phi^{s,t} &\leq \rho_{\phi, \mathcal{B}}^s \times d_{\mathcal{B}}(\Phi^s, \Phi^t) \\ &\leq \rho_\phi^s \times d_{\text{TV}}(\Phi^s, \Phi^t) \\ &\leq \log K \times d_{\text{TV}}(\Phi^s, \Phi^t).\end{aligned}$$

Proof. We have

$$\begin{aligned}\mu_\phi^{s,t} &= \int_{\Omega} \mathbb{H}(Y^s | \gamma^s) \mu^t(d\gamma) - \int_{\Omega} \mathbb{H}(Y^s | \gamma^s) \mu^s(d\gamma) \\ &= \sum_{B \in \mathcal{B}'} \Pr[\Phi^t \in B] \mathbb{H}(Y^s | \Phi^s \in B) - \sum_{B \in \mathcal{B}'} \Pr[\Phi^s \in B] \mathbb{H}(Y^s | \Phi^s \in B) \\ &= \sum_{B \in \mathcal{B}'} (\Pr[\Phi^t \in B] - \Pr[\Phi^s \in B]) \mathbb{H}(Y^s | \Phi^s \in B) \\ &\leq \sum_{B \in \mathcal{B}'} \max\{0, \Pr[\Phi^t \in B] - \Pr[\Phi^s \in B]\} \mathbb{H}(Y^s | \Phi^s \in B) \\ &\leq \sup_{B \in \mathcal{B}'} \mathbb{H}(Y^s | \Phi^s \in B) \times \sum_{B \in \mathcal{B}'} \max\{0, \Pr[\Phi^t \in B] - \Pr[\Phi^s \in B]\} \\ &= \sup_{B \in \mathcal{B}'} \mathbb{H}(Y^s | \Phi^s \in B) \times \frac{1}{2} \sum_{B \in \mathcal{B}'} |\Pr[\Phi^t \in B] - \Pr[\Phi^s \in B]| \\ &\leq \rho_{\phi, \mathcal{B}}^s \times d_{\mathcal{B}}(\Phi^s, \Phi^t).\end{aligned}$$

Clearly, $\rho_{\phi, \mathcal{B}}^s \leq \rho_\phi^s$. Let $U(\mathcal{B})$ be the family of sets that can be obtained by taking union of some sets in \mathcal{B} :

$$U(\mathcal{B}) = \{U : U = \cup_{B \in \mathcal{A}} B, \mathcal{A} \subseteq \mathcal{B}\}.$$

Then $d_{\mathcal{B}}(\mu, \nu) = \sup_{U \in U(\mathcal{B})} |\mu(U) - \nu(U)| \leq d_{\text{TV}}(\mu, \nu)$, where the last inequality follows from the definition of total variation distance. So the statement follows. \square

Algorithmic Implications. Note that both the point source fairness and group source fairness depend only on the source domain, and therefore one can hope to learn using labeled source data. Our results thus show that by encouraging fairness, that is, the accuracy being robust to change of source distributions, one can generalize better in view of covariate shift in domain adaptation problems. In fact, similar themes have been explored in some recent work, such as [11] (but which is not at representation level).

B Proofs in Section 4

B.1 Proof of Theorem 2

For any $e \in \mathcal{E}_{\text{tr}}$,

$$\begin{aligned}&R^{e_0}(f_\phi^e \circ \phi) - R^e(f_\phi^e \circ \phi) \\ &= \inf_{e' \in \mathcal{E}_{\text{tr}}} [R^{e_0}(f_\phi^e \circ \phi) - R^{e'}(f_\phi^e \circ \phi) + R^{e'}(f_\phi^e \circ \phi) - R^e(f_\phi^e \circ \phi)] \\ &\leq \inf_{e' \in \mathcal{E}_{\text{tr}}} [R^{e_0}(f_\phi^e \circ \phi) - R^{e'}(f_\phi^e \circ \phi)] + \sup_{e' \in \mathcal{E}_{\text{tr}}} [R^{e'}(f_\phi^e \circ \phi) - R^e(f_\phi^e \circ \phi)].\end{aligned}$$

Therefore, taking $\sup_{e \in \mathcal{E}_{\text{tr}}}$ on both sides and applying the max-min inequality leads to

$$\sup_{e \in \mathcal{E}_{\text{tr}}} R^{e_0}(f_\phi^e \circ \phi) \leq \sup_{e \in \mathcal{E}_{\text{tr}}} R^e(f_\phi^e \circ \phi) + d_\phi(e_0, \mathcal{E}_{\text{tr}}) + \sup_{e, e' \in \mathcal{E}_{\text{tr}}} [R^{e'}(f_\phi^e \circ \phi) - R^e(f_\phi^e \circ \phi)].$$

For the last term, using the same argument as in Theorem 1,

$$R^{e'}(f_\phi^e \circ \phi) - R^e(f_\phi^e \circ \phi) = \delta_\phi^{e, e'} + \text{KL}_\phi^{e, e'} + \mu_\phi^{e, e'}.$$

This completes the proof.

B.2 Proof of Proposition 1

Suppose the support of the target $\text{supp}(X^{e_0})$ can be disjoint from those of the sources $\cup_{e \in \mathcal{E}_s} \text{supp}(X^e)$, and let $v(x) = 0$ if x is from a source $e \in \mathcal{E}_s$ and $v(x) = 1$ if x is from the target e_0 . Suppose \mathcal{G} is large enough so that we have a $\phi \in \mathcal{G}$ that maps x to the concatenation of $\phi^*(x)$ and $v(x)$. Suppose f^* is linear and let \mathcal{F} be the set of linear functions, then we have an f with $f(\phi(x)) = f^*(\phi^*(x)) + 2v(x)$. Then for x from any source, $f(\phi(x)) = f^*(\phi^*(x))$, but for x from the target, $f(\phi(x)) = f^*(\phi^*(x)) + 2$. Suppose the target has an equal mass for the two class labels, then $h \circ \phi$ has source risks 0 but a large target risk $1/2$. Furthermore, it is easy to see that in all sources, ϕ^* satisfies ECI and the distributions of $\phi^*(X^e)$ are the same.

B.3 Distribution Memorization under Milder Assumptions

Proposition 1 shows large hypothesis classes can lead to too large predictor adaptation gap, but assuming the support of the target is disjoint with those of the sources. Here we show that this assumption is not needed in general, but just for the simplicity of the presentation and illustration of intuition.

Consider the following example. The input x lies on the real line. The conditional probability of the label $Y|X$ are the same for all domains: $Y = 0$ on $[-2, -1] \cup [1, 2]$, $Y = 1$ on $[-1, 1]$, and $\Pr[Y = 0|x] = \Pr[Y = 1|x] = 1/2$ for any $x \in [2, 3]$. The distributions of X are specified as follows.

1. The target domain e_0 puts uniformly mass ϵ on the interval $[-2, 0]$, mass ϵ on $[0, 2]$, and mass $1 - 2\epsilon$ on $[2, 3]$.
2. Source e_1 puts uniformly mass $1 - 2\epsilon$ on the interval $[-2, 0]$, mass ϵ on $[0, 2]$, and mass ϵ on $[2, 3]$.
3. Source e_2 puts mass ϵ on the interval $[-2, 0]$, mass $1 - 2\epsilon$ on $[0, 2]$, and mass ϵ on $[2, 3]$.

Then $\phi(x) = |x|$ and the classifier $f(\phi(x)) = \mathbf{1}[\phi(x) \leq 1]$ have the optimal error and satisfy ECI on the sources, but still has a large error $(1 - 2\epsilon)/2$ in the target domain. This is reflected by a large predictor adaptation gap. In this particular example, the gap is due to the covariate shift between the sources and the target (similar to the example in Proposition 1).

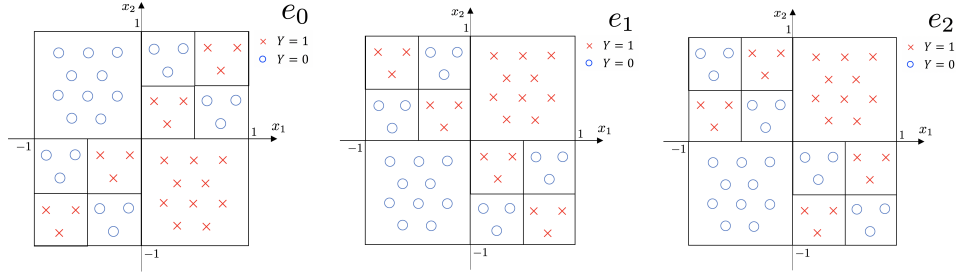


Figure 6: Illustrating example of distribution memorization: e_1 and e_2 are the two source environments, e_0 is the target environment. Both $\phi_1(x) = x_1$ and $\phi_2(x) = x_2$ satisfy the source ECI and zero source covariate shift. However, ϕ_2 will lead to a large target error.

Consider another example, shown in Figure 6. It is a variant of Example 1. The input space $\mathcal{X} = [-1, 1] \times [-1, 1]$, $\mathcal{G} = \{\phi_1, \phi_2\}$ where $\phi_1(x) = x_1$ and $\phi_2(x) = x_2$, and $\mathcal{F} = \{\mathbf{1}_\lambda(\cdot)\}$ (that is we consider thresholding functions that $\mathbf{1}_\lambda(\alpha) = 1$ if $\alpha > \lambda$, and 0 otherwise). The distributions are specified as follows. Let $\epsilon > 0$ be a sufficiently small constant.

1. The target e_0 puts uniformly mass $1/2 - \epsilon$ in the second and fourth quadrants, and mass ϵ in the first and third quadrants. It has label 1 for the fourth quadrant and label 0 for the second quadrant. In the first and third quadrant, it has label 1 for points in $[-1, -1/2] \times [-1, -1/2]$ or $[-1/2, 0] \times [-1/2, 0]$ or $[0, 1/2] \times [0, 1/2]$ or $[1/2, 1] \times [1/2, 1]$, and has label 0 for the other points.
2. Source e_1 puts uniformly mass $1/2 - \epsilon$ in the first and third quadrants, and mass ϵ in the second and fourth quadrants. It has label 1 for the first quadrant and label 0 for the third

quadrant. In the second and fourth quadrant, it has label 1 for points in $[-1, -1/2] \times [1/2, 1]$ or $[-1/2, 0] \times [0, 1/2]$ or $[0, 1/2] \times [-1/2, 0]$ or $[1/2, 1] \times [-1, -1/2]$, and has label 0 for the other points.

3. Source e_2 puts uniformly mass $1/2 - \epsilon$ in the first and third quadrants, and mass ϵ in the second and fourth quadrants. It has label 1 for the first quadrant and label 0 for the third quadrant. In the second and fourth quadrant, it has label 0 for points in $[-1, -1/2] \times [1/2, 1]$ or $[-1/2, 0] \times [0, 1/2]$ or $[0, 1/2] \times [-1/2, 0]$ or $[1/2, 1] \times [-1, -1/2]$, and has label 1 for the other points.

So both ϕ_1 and ϕ_2 lead to the optimal error and satisfy ECI in the sources. But ϕ_1 and the corresponding classifier $\mathbf{1}_0(\cdot)$ lead to a small error ϵ in the target, while ϕ_2 and the corresponding classifier $\mathbf{1}_0(\cdot)$ lead to a large error $1 - \epsilon$ in the target. Again, this is reflected by a large predictor adaptation gap. But in this particular example, the gap is due to the representation conditional label misalignment between the sources and the target.

In summary, both the representation conditional label misalignment and the covariate shift between the sources and the target can lead to a large predictor adaptation gap and consequently a large generalization gap, even when we can make sure the representation conditional label misalignment and the covariate shift among the sources are small. The precise relationship between the predictor adaptation gap and the misalignment/covariate shift between the sources and the target is left for future work.

C Relationship between ECI and IRM

Recall that the IRM approach proposed by [2] is to find $\hat{h}, \hat{\phi}$ by:

$$\min_{h \in \mathcal{F}, \phi \in \mathcal{G}} \sum_{e \in \mathcal{E}_{\text{tr}}} R^e(h \circ \phi), \quad (7)$$

$$\text{subject to } h \in \arg \min_{h \in \mathcal{F}} R^e(h \circ \phi) \text{ for any } e \in \mathcal{E}_{\text{tr}}. \quad (8)$$

This is empirical risk minimization subject to *simultaneous optimality* of the predictor for all sources. As pointed in [2], when the loss has the property that the minimizer is the Bayesian optimal predictor and \mathcal{F} is large enough to include that, ECI and simultaneous optimality are equivalent. Specifically we consider the following definition:

Definition 13 (ϕ -Bayesian Optimality Property). Let $\phi : \mathcal{X} \mapsto \mathcal{R}$ be a representation, $\ell : \Delta_K \times [K] \mapsto \mathbb{R}^+$ be a loss function, where $\Delta_K = \{(p_1, \dots, p_K) \mid p_i \geq 0, \sum_{i=1}^K p_i = 1\}$ is the K -dimensional probability simplex. Consider the following optimization problem:

$$\text{minimize}_{w: \mathcal{R} \rightarrow \Delta_K} \mathbb{E}[\ell(f(\phi(X)), Y)] \quad (9)$$

where the expectation is taken over X, Y . We say that ℓ has the Bayesian optimality property with respect to ϕ , if the optimal solution $f^* : \mathcal{R} \mapsto \Delta_K$ of (9), which maps a representation to a probability vector, satisfies that

$$\forall \gamma \in \text{supp}(\Phi), \forall y \in [K] : f^*(\gamma)_y = \Pr[Y = y \mid \Phi = \gamma]$$

Note that the simultaneous optimality is required for some $h \in \mathcal{F}$, while ECI or invariant predictor doesn't require h to be from \mathcal{F} . When the loss function has the Bayesian optimality property, ϕ satisfying ECI is equivalent to ϕ eliciting an invariant predictor (see the discussion later). We prefer to center our analysis around ECI rather than invariant predictor or simultaneous optimality for convenience, while simultaneous optimality is very useful for enforcing ECI in training.

Here, we analyze IRM under the following assumptions:

- (A1) The loss has the Bayesian optimality property.
- (A2) \mathcal{F} is sufficiently large to include the conditional probabilities $g(r) = \Pr(Y^e | \phi(X^e) = r)$ for any $\phi \in \mathcal{G}$ and any $e \in \mathcal{E}_{\text{tr}} \cup \{e_0\}$.

Under (A1)(A2), simultaneous optimality is equivalent to ϕ satisfying ECI.

It is worth noting many natural loss functions (e.g. squared loss, cross entropy) satisfies Bayesian optimality property. Combining (A1) and (A2), we have the following proposition:

Proposition 2. Let ϕ be a representation, ℓ be a loss function that satisfies the Bayesian optimality property w.r.t. ϕ , and \mathcal{E} be an environment family. Suppose that ϕ is conditionally invariant w.r.t. \mathcal{E} . Assuming (A2), then there is a universal optimal solution $f_\phi \in \mathcal{F}$ to the optimization problem $\min_h \mathbb{E}[\ell(h(\phi(X^e), Y^e))]$ across all $e \in \mathcal{E}$.

Proof. Define f_ϕ as

$$[f_\phi(r)]_y := [f_\phi^e(r)]_y = \Pr[Y^e = y \mid \phi(X^e) = r], y \in [K] \quad \text{for any } e \in \mathcal{E} \text{ that } \phi \in \text{supp}(\phi(X^e))$$

We note that f_ϕ is consistently defined because ϕ is conditionally invariant w.r.t. \mathcal{E} . Clearly, f_ϕ is optimal because ℓ satisfies Bayesian optimality property. \square

Now, given an environment family \mathcal{E} , and (A1) (A2) satisfied, by Proposition 2, we can consider the following objective:

$$\begin{aligned} & \underset{\phi}{\text{minimize}} \quad \sum_{e \in \mathcal{E}} \mathbb{E}[\ell(f_\phi(\phi(X^e)), Y^e)] \\ & \text{subject to } \text{ECI}(\phi, \mathcal{E}) \end{aligned} \quad \text{(ERM-ECI)}$$

Proposition 3. (ERM-ECI) is exactly the (IRM) objective defined as

$$\begin{aligned} & \underset{h, \phi}{\text{minimize}} \quad \sum_{e \in \mathcal{E}} \mathbb{E}[\ell(h(\phi(X^e)), Y^e)] \\ & \text{subject to } (\forall e \in \mathcal{E}) h \in \arg \min_{\bar{h}} \mathbb{E}[\ell(\bar{h}(\phi(X^e)), Y^e)] \end{aligned} \quad \text{(IRM)}$$

Proof. Because ℓ satisfies the conditional expectation property, therefore we know that for every $e \in \mathcal{E}$ the optimal solution will output the optimal conditional probability. Therefore for (IRM), the only possibility that there is an invariant optimal solution h across all environments, is that ϕ is conditionally invariant w.r.t. \mathcal{E} . However, then we know that the invariant optimal solution h in (IRM) is nothing but the f_ϕ . The proof is complete. \square

Without (A1)(A2), simultaneous optimality may not impose ECI; see an example in the next subsection.

C.1 Example Showing the Difference of ECI and IRM

C.1.1 Review of the colored-MNIST Experiment

In the paper [2], an interesting experiment on colored-MNIST is performed. The experiment is essentially as follows:

1. We start by considering a random variable G which encodes digits. Specifically, G is a random variable on \mathbb{R}^d of pixels. We abuse the notation to use G to denote the true digit its pixels encode (e.g. $G = 0$ means a sample that encodes 0).
2. We then define a Bernoulli random variable X as

$$X = \begin{cases} 0 & \text{if } G = 0, 1, 2, 3, 4, \\ 1 & \text{if } G = 5, 6, 7, 8, 9 \end{cases}$$

In other words, $X = 0$ if the digit encoded in G is less than 5, and 1 otherwise.

3. The true label Y is generated by flipping X with probability .25. That is,

$$Y = \begin{cases} X & \text{w.p. } .75, \\ 1 - X & \text{w.p. } .25 \end{cases}$$

In other words, the predictability⁶ of Y using X is $\Pr[X = Y] = .75$.

⁶ We define the *predictability* of a binary random variable Y using another binary random variable X as $\max\{\Pr[Y = X], \Pr[Y = 1 - X]\}$.

4. Then we create a *color random variable* Z , by flipping Y with probability q (define $p = 1 - q$). That is,

$$Z = \begin{cases} Y & \text{w.p. } p, \\ 1 - Y & \text{w.p. } q \end{cases}$$

That is, the predictability of Y using Z is p if $p > 1/2$, and q if $p \leq 1/2$.

5. Finally, after the color Z is sampled, we create a new pixel random variable \tilde{G} , by coloring the pixels of the digit in G using color Z (red if $Z = 0$ and green if $Z = 1$). Clearly, the causal structure is



Correlation between Y and Z is variant and thus is spurious. Note that both x and z can be recovered from \tilde{g} .

6. The task is to train a classifier to *predict* Y from \tilde{G} (that is a model $\tilde{G} \mapsto Y$). The experiment in [2] defines three environments: **(e₁)** where $q = .1$, which generates Z^{e_1} . Note that $\Pr[Y = Z^{e_1}] = .9 > .75 = \Pr[X = Y]$. **(e₂)** where $q = .2$, which generates Z^{e_2} . Note that $\Pr[Y = Z^{e_2}] = .8 > .75 = \Pr[X = Y]$. **(e₃)** (test environment): where $q = .9$, which generates Z^{e_3} . Note that now $\Pr[Y = Z^{e_3}] = .1 \ll .75 = \Pr[X = Y]$. That is, while in training environments Z is highly predictive, in the test environment it is poorly performing (and instead it is $1 - Z$ that is highly predictive).

IRM paper uses e_1 and e_2 for training. It is straightforward now to instantiate both (IRM) and (IRMv1) objectives with the above setting. Interestingly, with (IRMv1), [2] found that they can learn to use X , but not Z . In a nutshell, they claim that, even with the following two assumptions:

1. The correlation between Y and Z *varies* over training environments.
2. In every training environment Z is more predictive than X in predicting Y .

IRM can still learn *not* to use correlations that are *not* invariant.

C.1.2 Example where IRM Does Not Impose ECI

We now prove that if we use the 0-1 loss (which does not have the Bayesian optimality property), then the optimal solutions to (IRM) in color-MNIST do not satisfy ECI and should learn the spurious correlation Z (i.e., the color).

To start with, we consider 0-1 loss, that is, given hypothesis h that maps $g \sim \tilde{G}$ to $\{0, 1\}$,

$$\ell(g, y; h) = \mathbb{1}[h(g) \neq y] = \begin{cases} 1 & h(g) \neq y, \\ 0 & \text{otherwise.} \end{cases}$$

and therefore $R^e(h)$ is defined to be $\sum_{(g,y) \sim \tilde{G}^e} \ell(g, y; h)$.

Our construction has two steps: First, we construct one optimal solution (Φ^*, w^*) to (IRM), but which learns the spurious correlation Z . Second, we prove that *any* optimal solution should learn the spurious correlation Z .

Constructing an optimal (Φ^*, w^*) to (IRM). Now, we construct representation Φ^* and classifier w^* :

- We let Φ^* be the representation that maps a colored image $g \sim \tilde{G}$ to a binary vector in $\{0, 1\}^2$:

$$\Phi^*(\tilde{G}) = \begin{bmatrix} X \\ Z \end{bmatrix}$$

That is, from \tilde{G} , Φ^* optimally reconstructs the digit concept X and color concept Z .

- We construct classifier w^* as

$$w^* = \begin{bmatrix} 0 \\ 1 \end{bmatrix}$$

In other words, $(w^*)^\top \Phi^*(\tilde{G}) = Z$, which simply outputs the color concept.

We have the following proposition,

Proposition 4. For 0-1 loss, (Φ^*, w^*) is an optimal solution to (IRM). Specifically, outputting color Z using w^* is optimal in e_1 and e_2 respectively, and achieves minimal empirical risk combining environments e_1 and e_2 .

Proof. Consider the Bayesian optimal classifier c^* given X, Z . That is

$$c^*(x, z) = \begin{cases} 1 & \text{if } \Pr[Y = 1|x, z] > 1/2 \\ 0 & \text{otherwise.} \end{cases}$$

For any predictor $f : \tilde{G} \mapsto \{0, 1\}$, we show that $\Pr[Y \neq f(\tilde{G})] \geq \Pr[Y \neq c^*(X, Z)]$. That is $c^*(X, Z)$ achieves the optimal error among all predictors over \tilde{G} . To see this, note that from **(Causal Structure)**, we have that $Y \perp\!\!\!\perp \tilde{G} \mid (X, Z)$. Thus $Y \perp\!\!\!\perp f(\tilde{G}) \mid (X, Z)$. Therefore by the law of total expectation

$$\begin{aligned} \Pr[Y \neq f(\tilde{G})] &= \mathbb{E}_{X, Z}[\mathbb{E}[\mathbb{1}\{Y \neq f(\tilde{G})\} \mid X, Z]] \\ &= \sum_{x, z} p(x, z) \cdot \left(p(Y = 1, f(\tilde{G}) = 0 \mid x, z) + p(Y = 0, f(\tilde{G}) = 1 \mid x, z) \right) \\ &= \sum_{x, z} p(x, z) \cdot \left(p(Y = 1|x, z)p(f(\tilde{G}) = 0|x, z) + p(Y = 0|x, z)p(f(\tilde{G}) = 1|x, z) \right) \\ &\geq \sum_{x, z} p(x, z) \cdot \min \left\{ p(Y = 1|x, z), p(Y = 0|x, z) \right\} \\ &= \sum_{x, z} p(x, z) \cdot \Pr[Y \neq c^*(x, z)] \\ &= \Pr[Y \neq c^*(X, Z)] \end{aligned}$$

Clearly, $\Phi^*(\tilde{G}) = (X, Z)$. Next we show that $c^* = w^*$. For each environment we can compute the Bayesian optimal predictor $\Pr[Y = y \mid X = x, Z = z]$, for $x, y, z \in \{0, 1\}$. We have that,

e_1	$y = 0$	$y = 1$	e_2	$y = 0$	$y = 1$
$x = 0, z = 0$	$\frac{27}{28}$	$\frac{1}{28}$	$x = 0, z = 0$	$\frac{12}{13}$	$\frac{1}{13}$
$x = 0, z = 1$	$\frac{1}{4}$	$\frac{3}{4}$	$x = 0, z = 1$	$\frac{3}{7}$	$\frac{4}{7}$
$x = 1, z = 0$	$\frac{3}{4}$	$\frac{1}{4}$	$x = 1, z = 0$	$\frac{4}{7}$	$\frac{3}{7}$
$x = 1, z = 1$	$\frac{1}{28}$	$\frac{27}{28}$	$x = 1, z = 1$	$\frac{1}{13}$	$\frac{12}{13}$

For each row, we highlight (bold) the cell which Bayesian optimal predictor should output. One can see that for either environment, the Bayesian optimal predictor is simply to output z . This shows that:

- z is the optimal predictor for e_1 and e_2 , respectively, and,
- The Bayesian optimal predictor for e_1 and e_2 together is also simply z .

We note that $w^* \circ \Phi^*$ gives the optimal predictor z , and also that w^* is the optimal hypothesis for $\Phi^*(\tilde{G}^{e_1})$ and $\Phi^*(\tilde{G}^{e_2})$, respectively. Therefore (w^*, Φ^*) is an optimal solution to (IRM). \square

From “an” optimal solution to “any” optimal solution. We have the following:

Proposition 5. For 0-1 loss, and any optimal solution $\bar{\Phi}, \bar{w}$ to (IRM), $\bar{w} \circ \bar{\Phi}$ must be Z (i.e., the color).

Proof. Consider any optimal solution $\bar{\Phi}$ and \bar{w} to (IRM). It must satisfy that its empirical loss across all environments must be upper bounded by that of Φ^* and w^* . That is,

$$R^{e_1}(\bar{w} \circ \bar{\Phi}) + R^{e_2}(\bar{w} \circ \bar{\Phi}) \leq R^{e_1}(w^* \circ \Phi^*) + R^{e_2}(w^* \circ \Phi^*).$$

However $w^* \circ \Phi^*$ is the Bayesian optimal predictor Z . This means that $\bar{w} \circ \bar{\Phi}$ must also be Z . The proof is complete. \square

Combining Propositions 4 and 5 it shows that (IRM) cannot impose ECI and learn invariant correlations.

D Experimental Details for IRM under Representation Covariate Shift

There are two training environments e_1, e_2 and one testing environment e_0 . The data is generated with two control parameter p, n as follows: We first we assign a preliminary label $\tilde{y} = 0$ for digit 0 – 4, and $\tilde{y} = 1$ for digit 5 – 9 for each data point in MNIST. Then to create e_1, e_2 , we randomly partition the 50000 MNIST training samples into two sets S_1 and S_2 . In e_1 , we sample n points with replacement from set S_1 to obtain data from 0-4 with probability $\frac{p}{1+p}$ and data from 5-9 with probability $\frac{1}{1+p}$; in e_2 , we sample n points with replacement from set S_2 to obtain data from 0-4 with probability $\frac{1}{1+p}$ and data from 5-9 with probability $\frac{p}{1+p}$. Finally, we create final label (true label) for data in all environments, y , by flipping \tilde{y} with probability 0.25. Finally, we create the color variable

for each sample c by flipping y with probability q^e , where $q^e = \begin{cases} 0.2 & e = e_1 \\ 0.1 & e = e_2 \\ 0.9 & e = e_0 \end{cases}$.

The result is given in Table 1. We can observe that as n increases, the train accuracy-test accuracy gap shrinks. As p decreases, the training accuracy increases steadily. The test accuracy drops significantly in particular when p goes from 0.6 to 0.3. The reason, we think, is that the IRM is no longer able to learn a useful representation from the two training environments with completely misaligned feature representations.

E More Related Work

Representation learning has become a popular approach for various applications, and learning invariant representations across multiple domains has been a popular method for domain adaptation in recent years. A classic approach for analyzing domain adaption is based on \mathcal{H} -divergence [15, 7, 4]. That theoretical framework is the basis for a line of methods that uses adversarial training with neural networks to learn representations that are indistinguishable between source and target domain, in particular domain adversarial neural network (DANN) [1, 12] and related techniques [21, 30]. Some other approach used different divergence notions, such as MMD [18, 17], Wasserstein distance [8, 27], and Rényi divergence [19]. Another line of research for domain adaptation is based on causal approaches that typically assume shared generative distributions, e.g., [28, 13, 3]. This work instead focuses on discriminative representation learning and does not make generative assumptions.

On the other hand, the \mathcal{H} -divergence bound is for general learning rather than representation learning, and thus falls short in explaining some failure cases. To this end, our bounds are finer-grained than the classic bounds for domain adaptation based on \mathcal{H} -divergence, e.g., that by [4]. For single source, a similar bound as Theorem 1 can be derived from the classic \mathcal{H} -divergence based bound, by bounding the \mathcal{H} -divergence by the label divergence and covariate shift. On the other hand, the bound in Theorem 1 is tighter (it is an *equality!*) and the analysis is more intuitive. For multiple sources, we can also derive a multi-source \mathcal{H} -divergence based bound. Our multi-source bound can also be viewed as decomposing the \mathcal{H} -divergence into finer-grained quantities. See Section F in the appendix for the details.

Invariant Risk Minimization (IRM) [2] proposed to learn representations that result in the same optimal prediction across domains. We noted that this corresponds to enforcing one factor in our risk decomposition, which also reveals conditions for success and suggests potential improvements to IRM.

p	n	Training accuracy (std dev.)	Test accuracy (std dev.)
1	25000	0.7141 (0.0095)	0.6489 (0.0163)
1	50000	0.6978 (0.0057)	0.6955 (0.0079)
1	100000	0.6995 (0.0057)	0.6986 (0.0099)
0.9	25000	0.7193 (0.0126)	0.6578 (0.0158)
0.9	50000	0.7059 (0.0056)	0.6951 (0.0136)
0.9	100000	0.7033 (0.0053)	0.7087 (0.0092)
0.8	25000	0.7152 (0.0072)	0.6823 (0.0121)
0.8	50000	0.7107 (0.0053)	0.6986 (0.0071)
0.8	100000	0.7067 (0.0054)	0.7025 (0.0092)
0.7	25000	0.7347 (0.0122)	0.6437 (0.0316)
0.7	50000	0.7254 (0.0055)	0.6724 (0.0124)
0.7	100000	0.7198 (0.0032)	0.6797 (0.0077)
0.6	25000	0.7512 (0.0115)	0.6126 (0.038)
0.6	50000	0.7419 (0.0047)	0.6332 (0.013)
0.6	100000	0.7343 (0.0056)	0.6388 (0.0161)
0.5	25000	0.7767 (0.013)	0.4915 (0.0583)
0.5	50000	0.7551 (0.0067)	0.5885 (0.0271)
0.5	100000	0.7519 (0.0084)	0.5981 (0.039)
0.4	25000	0.7916 (0.0241)	0.4089 (0.0991)
0.4	50000	0.7828 (0.0152)	0.4441 (0.0715)
0.4	100000	0.7739 (0.0073)	0.5053 (0.0392)
0.3	25000	0.8356 (0.0065)	0.2457 (0.0257)
0.3	50000	0.8261 (0.0152)	0.2756 (0.0497)
0.3	100000	0.8277 (0.0078)	0.2668 (0.0286)
0.2	25000	0.8463 (0.0021)	0.1879 (0.0095)
0.2	50000	0.8444 (0.001)	0.1801 (0.0067)
0.2	100000	0.8425 (0.001)	0.1853 (0.0054)
0.1	25000	0.8465 (0.0017)	0.1901 (0.0109)
0.1	50000	0.8459 (0.0009)	0.1717 (0.0127)
0.1	100000	0.8455 (0.0007)	0.1665 (0.0082)

Table 1: Complete results of IRM under covariate shift. The covariate shift is created by manipulation of the data distribution described in the text in Section D.

F Relations between Our Bounds and Divergence-based Bounds

F.1 Review of the Divergence-based Bound for Single-Source Domain Adaptation

The seminal work by [4] considered the setting of single-source domain adaptation without representation learning, i.e., only considering \mathcal{H} but not \mathcal{F} or \mathcal{G} . It gives a bound on the risk in the target domain, based on the notion of \mathcal{H} -divergence. We review the divergence and the bound below.

By learning on the source, one cannot hope the learned hypothesis to generalize to arbitrary target. Therefore, some criterion is needed to measure how close the target is to the source. A naive measurement is the L_1 distance. However, [4] pointed out the L_1 distance cannot be accurately estimated from finite samples of arbitrary distributions. Furthermore, it is a supremum over all measurable subsets while we are only interested in the risk of hypothesis from a class of finite complexity. They thus proposed to use the \mathcal{H} -divergence instead. The original bound is derived for the setting where the label $y \in [0, 1]$, the output of the hypothesis is in $\{0, 1\}$, and the loss is $\ell(y, y') = |y - y'|$. Here we give a variant of the divergence and the original bound for general loss, which is convenient for the later discussion on comparison to our bounds.

Definition 14. Denote the difference between the risks of two hypotheses h, h' as

$$v_e(h, h') = |R^e(h) - R^e(h')|. \quad (10)$$

The generalized $\mathcal{H}\Delta\mathcal{H}$ -divergence between two distributions e, e' is

$$d_{\mathcal{H}\Delta\mathcal{H}}(e, e') = 2 \sup_{h, h' \in \mathcal{H}} |v_e(h, h') - v_{e'}(h, h')|. \quad (11)$$

The generalized divergence upper bounds the change of the hypothesis risk difference due to distribution shifts. If it is small, then for any $h, h' \in \mathcal{H}$ where h has a smaller risk than h' in e , we know that h will also have a smaller (or not too larger) risk than h' in e' . That is, if the divergence is small, then the ranking of the hypotheses w.r.t. the risk is roughly the same in both distributions. This *rank-preserving* property makes sure that a good hypothesis learned in one domain will also be good for another.

Theorem 5. *Suppose the loss is non-negative. For any $h \in \mathcal{H}$,*

$$R^t(h) \leq \inf_{h^* \in \mathcal{H}} \{R^t(h^*) + R^s(h^*)\} + R^s(h) + d_{\mathcal{H}\Delta\mathcal{H}}(s, t). \quad (12)$$

Proof. By definition of $d_{\mathcal{H}\Delta\mathcal{H}}(s, t)$ and non-negativity of the loss,

$$d_{\mathcal{H}\Delta\mathcal{H}}(s, t) \quad (13)$$

$$\geq \sup_{h^* \in \mathcal{H}} \{|v_t(h, h^*) - v_s(h, h^*)|\} \quad (14)$$

$$\geq \sup_{h^* \in \mathcal{H}} \{R^t(h) - R^t(h^*) - R^s(h) + R^s(h^*)\}. \quad (15)$$

Rearranging the terms completes the proof. \square

F.2 Comparing Our Single-Source Bound to the Divergence-based Bound

We can derive a bound by first applying the divergence-based bound Theorem 5 on the hypothesis class $\mathcal{H} = \{f_\phi^s \circ \phi, f_\phi^t \circ \phi\}$, and then bounding the divergence with our notions $\text{KL}_\phi^{s,t}, \text{KL}_\phi^{t,s}, \delta_\phi^{s,t}$, and $\mu_\phi^{s,t}$.

Proposition 6.

$$R^t(f_\phi^s \circ \phi) \leq 3R^s(f_\phi^s \circ \phi) + \max\{\text{KL}_\phi^{s,t}, \text{KL}_\phi^{t,s}\} + \delta_\phi^{s,t} + \mu_\phi^{s,t}.$$

Proof. Recall $\text{KL}_\phi^{t,s} = R^s(f_\phi^t \circ \phi) - R^s(f_\phi^s \circ \phi)$ and $\text{KL}_\phi^{s,t} = R^t(f_\phi^s \circ \phi) - R^t(f_\phi^t \circ \phi)$. Applying the divergence-based bound Theorem 5 on the hypothesis class $\mathcal{H} = \{f_\phi^s \circ \phi, f_\phi^t \circ \phi\}$ gives:

$$R^t(f_\phi^s \circ \phi) \leq R^s(f_\phi^s \circ \phi) + \min_{h \in \mathcal{H}} \{R^s(h) + R^t(h)\} + |\text{KL}_\phi^{t,s} - \text{KL}_\phi^{s,t}|.$$

If $\text{KL}_\phi^{t,s} \geq \text{KL}_\phi^{s,t}$, then

$$\begin{aligned} \min_{h \in \mathcal{H}} \{R^s(h) + R^t(h)\} + |\text{KL}_\phi^{t,s} - \text{KL}_\phi^{s,t}| &\leq \text{KL}_\phi^{t,s} - \text{KL}_\phi^{s,t} + R^s(f_\phi^s \circ \phi) + R^t(f_\phi^s \circ \phi) \\ &\leq \text{KL}_\phi^{t,s} + R^s(f_\phi^s \circ \phi) + R^t(f_\phi^t \circ \phi). \end{aligned}$$

If $\text{KL}_\phi^{t,s} \leq \text{KL}_\phi^{s,t}$, then

$$\begin{aligned} \min_{h \in \mathcal{H}} \{R^s(h) + R^t(h)\} + |\text{KL}_\phi^{t,s} - \text{KL}_\phi^{s,t}| &\leq -\text{KL}_\phi^{t,s} + \text{KL}_\phi^{s,t} + R^s(f_\phi^t \circ \phi) + R^t(f_\phi^t \circ \phi) \\ &\leq \text{KL}_\phi^{s,t} + R^s(f_\phi^s \circ \phi) + R^t(f_\phi^t \circ \phi). \end{aligned}$$

Then the statement follows from $R^t(f_\phi^t \circ \phi) - R^s(f_\phi^s \circ \phi) = \delta_\phi^{s,t} + \mu_\phi^{s,t}$. \square

Our bound in Theorem 1 is an equality and thus tighter than this, and the proof is simpler and more intuitive. The above proposition also shows that our bound gives a finer-grained analysis than the divergence-based bound Theorem 5.

It is also instructive to apply Theorem 5 to explain Example 1. If we apply it to $\mathcal{H} = \mathcal{F} \circ \mathcal{G}$, then we can see that the first two terms $\inf_{h^* \in \mathcal{H}} \{R^t(h^*) + R^s(h^*)\}$ and $R^s(h)$ can be small. However, $d_{\mathcal{H}\Delta\mathcal{H}}(s, t)$ will be large. Therefore, the bound can detect that the learned model may not generalize to the target domain, but it doesn't point out what leads to the problem, while our bound points out that the representation conditional label misalignment does. Furthermore, the subtle issue in Example 1 arises when one applies Theorem 5 on the representation level instead of the input level. More precisely, if we apply it on $\mathcal{H}_1 = \mathcal{F} \circ \{\phi_1\}$, we have

$$R^t(f \circ \phi_1) \leq \inf_{f^* \in \mathcal{F}} \{R^t(f^* \circ \phi_1) + R^s(f^* \circ \phi_1)\} + R^s(f \circ \phi_1) + d_{\mathcal{H}_1\Delta\mathcal{H}_1}(s, t). \quad (16)$$

Similarly, if we apply it on $\mathcal{H}_2 = \mathcal{F} \circ \{\phi_2\}$, we have

$$R^t(f \circ \phi_2) \leq \inf_{f^* \in \mathcal{F}} \left\{ R^t(f^* \circ \phi_2) + R^s(f^* \circ \phi_2) \right\} + R^s(f \circ \phi_2) + d_{\mathcal{H}_2 \Delta \mathcal{H}_2}(s, t). \quad (17)$$

The last two terms can be made small, but the generalization gap gets hidden in the first term. In particular, both $d_{\mathcal{H}_1 \Delta \mathcal{H}_1}(s, t)$ and $d_{\mathcal{H}_2 \Delta \mathcal{H}_2}(s, t)$ are 0, but $d_{\mathcal{H} \Delta \mathcal{H}}(s, t)$ can be large. Note that though $\mathcal{H} = \mathcal{H}_1 \cup \mathcal{H}_2$, $d_{\mathcal{H} \Delta \mathcal{H}}(s, t)$ is much larger than the maximum of $d_{\mathcal{H}_1 \Delta \mathcal{H}_1}(s, t)$ and $d_{\mathcal{H}_2 \Delta \mathcal{H}_2}(s, t)$. The difference between $d_{\mathcal{H} \Delta \mathcal{H}}(s, t)$ and $\max\{d_{\mathcal{H}_1 \Delta \mathcal{H}_1}(s, t), d_{\mathcal{H}_2 \Delta \mathcal{H}_2}(s, t)\}$ gets hidden in the first term, and is the root for the subtle issue in Example 1. In summary, using the bound on the input level is the correct way to apply it, which can detect there is an issue for generalization but still doesn't point out where the issue comes from.

F.3 Generalizing the Divergence-based Bound to Multi-Source Domain Adaptation

Here we show one can generalize the divergence-based bound for the case with a single source s and target t to the case with multiple sources \mathcal{E}_{tr} and a target e_0 .

Based on the divergence, we introduce the key notion for the analysis:

Definition 15. *The \mathcal{H} -misalignment from e_0 to \mathcal{E}_{tr} is*

$$d_{\mathcal{H}}(e_0; \mathcal{E}_{\text{tr}}) = \inf_{e \in \mathcal{E}_{\text{tr}}} \left\{ \frac{1}{2} d_{\mathcal{H} \Delta \mathcal{H}}(e_0, e) \right\} = \inf_{e \in \mathcal{E}_{\text{tr}}} \sup_{h, h' \in \mathcal{H}} |v_{e_0}(h, h') - v_e(h, h')|. \quad (18)$$

The notion measures how aligned e_0 is to \mathcal{E}_{tr} w.r.t. risk ranking. Intuitively, as long as there exists one $e \in \mathcal{E}_{\text{tr}}$ whose ranking of the hypotheses by their risks is similar to that of e_0 , then e_0 is aligned to \mathcal{E}_{tr} . To emphasize the difference from typical distribution distances, we use the term misalignment instead.

Then we can generalize Theorem 5 as follows.

Theorem 6. *Suppose the loss is non-negative. For any e_0 and any $h \in \mathcal{H}$,*

$$R^e(h) \leq \inf_{h^* \in \mathcal{H}} \left\{ R^{e_0}(h^*) + \sup_{e \in \mathcal{E}_{\text{tr}}} R^e(h^*) \right\} + \sup_{e \in \mathcal{E}_{\text{tr}}} R^e(h) + d_{\mathcal{H}}(e_0; \mathcal{E}_{\text{tr}}). \quad (19)$$

Proof. By definition of $d_{\mathcal{H}}(e_0; \mathcal{E}_{\text{tr}})$ and non-negativity of the loss,

$$d_{\mathcal{H}}(e_0; \mathcal{E}_{\text{tr}}) \quad (20)$$

$$\geq \inf_{e \in \mathcal{E}_{\text{tr}}} \sup_{h^* \in \mathcal{H}} \{|v_{e_0}(h, h^*) - v_e(h, h^*)|\} \quad (21)$$

$$\geq \inf_{e \in \mathcal{E}_{\text{tr}}} \sup_{h^* \in \mathcal{H}} \{R^{e_0}(h) - R^{e_0}(h^*) - R^e(h) + R^e(h^*)\}. \quad (22)$$

Applying the maxmin inequality and then rearranging the terms completes the proof. \square

Similar to the single-source case, the bound in Theorem 6 uses $\inf_{h^* \in \mathcal{H}} \{R^{e_0}(h^*) + \sup_{e \in \mathcal{E}_{\text{tr}}} R^e(h^*)\}$ and $d_{\mathcal{H}}(e_0; \mathcal{E}_{\text{tr}})$. While our bound in Theorem 2 uses our notions of representation conditional label divergence, representation covariate shift, and prediction adaptation gap. The terms in Theorem 6 can also be bounded using our notions using a similar argument as in Proposition 6. Therefore, compared to the divergence-based bound, our bound provides a finer-grained analysis in the setting of representation learning.